Damage of low-energy ion irradiation on copper nanowire: molecular dynamics simulation*

Zou Xue-Qing(邹雪晴)[a], Xue Jian-Ming(薛建明)[a)b)†], and Wang Yu-Gang(王宇钢)[a]

[a] *State Key Laboratory of Nuclear Physics and Technology, School of Physics, Peking University, Beijing* 100861, *China*
[b] *Center for Applied Physics and Technology, Peking University, Beijing* 100861, *China*

(Received 14 March 2009; revised manuscript received 26 August 2009)

Physical and chemical phenomena of low-energy ion irradiation on solid surfaces have been studied systematically for many years, due to the wide applications in surface modification, ion implantation and thin-film growth. Recently the bombardment of nano-scale materials with low-energy ions gained much attention. Comared to bulk materials, nano-scale materials show different physical and chemical properties. In this article, we employed molecular dynamics simulations to study the damage caused by low-energy ion irradiation on copper nanowires. By simulating the ion bombardment of 5 different incident energies, namely, 1 keV, 2 keV, 3 keV, 4 keV and 5 keV, we found that the sputtering yield of the incident ion is linearly proportional to the energies of incident ions. Low-energy impacts mainly induce surface damage to the nanowires, and only a few bulk defects were observed. Surface vacancies and adatoms accumulated to form defect clusters on the surface, and their distribution are related to the type of crystal plane, e.g. surface vacancies prefer to stay on (100) plane, while adatoms prefer (110) plane. These results reveal that the size effect will influence the interaction between low-energy ion and nanowire.

Keywords: low-energy ion, irradiation, nanowire, molecular dynamics simulation
PACC: 6146, 6185, 7920

1. Introduction

Nanowires are widely used as blocks for nanodevices, ranging from chemical and biological sensors to logic circuits.[1,2] Due to the size effect, the structural properties of nanowires including atomic arrangement, morphology and defects distribution of the system play fundamental roles in determining the physical attributes (optical, mechanical and electrical) of nanowires.[3−6]

Low-energy ion irradiation has modification effects on the surface or near surface of the solid, so it is ubiquitously employed in the modification of surface structure, thin-film growth, and various types of surface analysis techniques.[7−9] The bulk and surface damages induced by the dissipation of the incident ion's energy involve metastable phases and isolated defects formation.[10] As for the nanowire, these damages caused by ion bombardment are comparable to the size of the nanowire itself, which can greatly change its structural properties.[11] Though the ion irradiation on metallic and semiconductor bulk material has been widely studied,[12−15] ion irradiation on metal nanowires is seldom researched. Some papers studied the effect of existed defects on physical properties of nanowires,[3] but researches on the formation and movement of defects induced by irradiation are lack. Due to the size effect, the interaction of energetic ions with nanowires gives rise to different physical phenomena from the traditional theories, i.e. the increase of sputtering yield. Moreover, the surface relaxation which is surface-orientation dependent[16] may induce some different phenomena on nanowire.

In the present work, we conducted molecular dynamics simulation to study the physical phenomenon of low-energy ion bombardment with 3 nm-diametre copper nanowires. In nanowire system, the sputtering yield increases linearly with the rise of energy of incident ion, which is unlike the bulk system (sputtering yield slows down after a threshold energy value). With the increase of energy of incident ion, the defects distributed all around the nanowire, not only the incident side. Computational simulation also elucidated the process of accumulation of surface vacancies adatoms, and recombination of defect. Furthermore, the distribution of defects showed that surface vacancies favour (100) plane, while adatoms favour (110) plane.

*Project supported by the National Natural Science Foundation of China (Grant No. 10675009).
†Corresponding author. E-mail: jmxue@pku.edu.cn
© 2010 Chinese Physical Society and IOP Publishing Ltd

2. Simulation methods

2.1. System setup and molecular dynamics

Copper nanowire used in simulation was a 30 Å-diametre (1 Å=0.1 nm) octahedron built from a block of fcc single crystal using cutoff diametre (30 Å) for the simulation. The eight sides of nanowire involves four (100) crystal plane and four (110) crystal planes, see Fig. 1. The axial of nanowires is along ⟨001⟩ crystalline direction. Incident copper ion was placed 20 Å away from nanowire. Incident copper ion with kinetic energies E varied between 1 and 5 keV at 1 keV intervals impacts on the (100) crystal plane of nanowire from ⟨135⟩ crystal direction. The nanowire contains 5400 atoms in total.

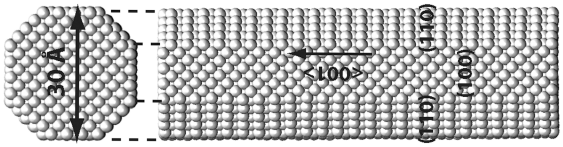


Fig. 1. Atomic view of nanowire.

The simulations were conducted by MD program developed by our lab with the Ziegler–Biersack–Littmark (ZBL) universal repulsive potential[17] and embedded atom method (EAM) potential of Mishin *et al.*[18,19] ZBL potential was used to describe the interaction between recoil atom and its neighbours, and the other atoms used EAM potential. Periodic boundary condition was used along the axial direction. The sides of the nanowire represented a free surface towards vacuum, and was allowed to relax freely. In our simulation, we did not apply electron–phonon coupling, since the ion energies were very low and the electronic energy loss could be negligible to the low incident energy ($\leq$ 5 keV). The cutoff of EAM potential used in simulation is 6.5 Å, and cutoff of ZBL potential is 10.5 Å.

For each simulation, we minimized the system for 1 ps to obtain the optimized geometry of nanowires, and then heat the sample to 100K in 1 ps. The system was equilibrated at 100 K for 30 ps by using Nose–Hoover thermostat method before irradiation. Five energies of incident ions were simulated: 1 keV, 2 keV, 3 keV, 4 keV and 5 keV. During cascade evolution, atoms involved in cascade collision were not applied thermostat coupling to avoid disturbing the irradiation process.[20] The timestep for integration of equations of motion during collision stage is 0.01 fs. In each run, incident ion impinged with random coordinates. The total simulation time varies for each incident energy. For 1 keV and 2 keV impacts, simulations last 6 ps. For 3 keV, 4 keV and 5 keV impacts, simulations last 10 ps, 12 ps and 16 ps respectively.

2.2. Analysis methods

We collected the number of sputtered atoms, vacancy, interstitials and adatoms to analysis the irradiation damage on nanowire. The sputtered atoms are those which ran 2 nm away from the surface of nanowires. Due to the small size of nanowire, all atoms of nanowire are close to the surface, it is difficult to distinguish exactly surface vacancy from bulk vacancy, and adatom from interstitial during irradiation process. In our simulations, we consider surface vacancy as part of vacancy. By comparing the irradiated nanowire with the original fcc crystal structure, the vacancy is defined as an atomic site where there is no atom within the distance of 1 Å.[21] An interstitial is defined as an extra atom located 1 Å away to the nearest atomic site.[21] An adatom is an especial interstitial on the surface of crystallite.

3. Results

3.1. Energy dependent structural damage of nanowire

Bombardment of energetic ion induces displacement of atoms in nanowires. Sputtered atoms, bulk vacancies, interstitials, surface vacancies and adatoms were observed during the irradiation process. The morphology of nanowire surface was greatly modified by the formation of defects. Figure 2 illustrates the final damage states of nanowire surface caused by incident ion with 5 different energies. Under 1 keV incident energy, a few of surface vacancies and adatoms formed on the surface. A small and shallow nanogroove formed by a cluster of surface vacancies was observed. This surface vacancies only involved on the first layer. Under 1 keV-bombardment, all surface defects were only found on the incident face of energetic ion. With the increase of incident ion's energy, three distinguish features were observed on damaged

nanowire: (i) nanogrooves become deeper. Surface vacancies are not only observed on the first layer, but also on the second or even on the third layer. Figure 3(b) demonstrates that under 2 keV, the surface vacancy cluster involves 3 atomic layers. (ii) the defects including surface vacancies and adatoms spread from the incident side to all sides around the nanowire, see Fig. 3. Under 1 keV, the defects only located around the incident point of ion. With the increase of ion energy, the damage involves larger surface areas of nanowire. Under 5 keV bombardment, defects distribute all over the cylindrical surface of nanowire. (iii) under higher-energy impact, bulk defects (vacancy and interstitial) were observed in the nanowire. A single vacancy was formed inside of nanowire, under 3 keV and 4 keV-bombarments (as shown in Fig. 3(c) and Fig. 3(d)). Although in our limited simulations, the probability of bulk defects occuring is low, this trend indicates that higher incident energy can extend the surface damage to the inside bulk damage.

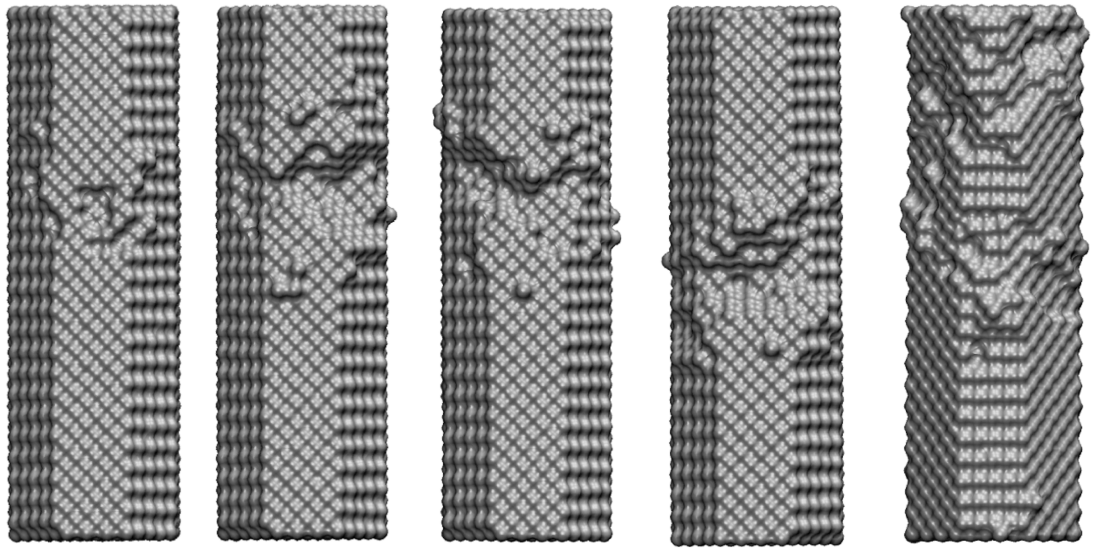


Fig. 2. Atomic views of nanowire surface morphologies resulting after Cu ion bombardment. (a) 1 keV, (b) 2 keV, (c) 3 keV, (d) 4 keV, (e) 5 keV. 1 keV bombardment resulted in a few damage on the incident surface. More surface defects were induced by increasing incident energy, and surface defects diffused from the incident surface to the surfaces all around nanowire. Furthermore, the distribution of surface defects is crystalline surface dependent, namely, vacancies accumulated on ⟨100⟩ plane, while adatoms accumulated on ⟨110⟩ plane.

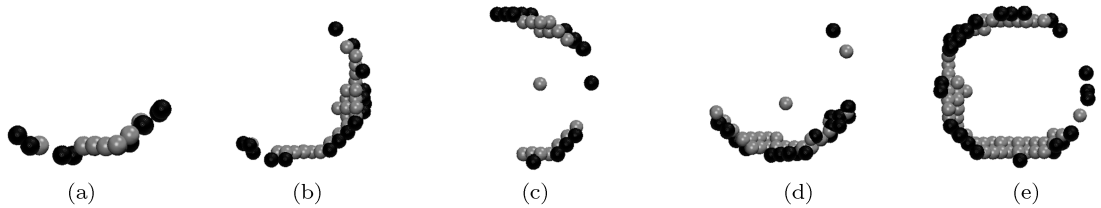


Fig. 3. Top view of defects distribution in nanowire. (a) 1 keV, (b) 2 keV, (c) 3 keV, (d) 4 keV, (e) 5 keV. Vacancy (grey) sites and adatom (black) sites are explicitly shown. Under 1 keV, the defects only located around the incident point of ion on the surface. With the increase of incident energy, the damage involves more and more surface areas of nanowire around. The defects induced by ion bombardment eventually diffused to the surface of nanowire, few defects were found inside the nanowire. Under 3 keV and 4 keV ion bombardment, only one vacancy were observed inside the nanowire, which indicates that increasing incident energy may cause damage inside the nanowire.

3.2. Sputtering from copper nanowire

In all simulations, a plenty of sputtered atoms were generated during ion bombardment. Figure 4 presents the sputtering yield of Cu ion impacting copper nanowire in ⟨135⟩ direction, together with the mean value and

standard error bars for each incident energy at 100 K. The sputtering yield increases almost linearly with the rise of incident ion's energy.

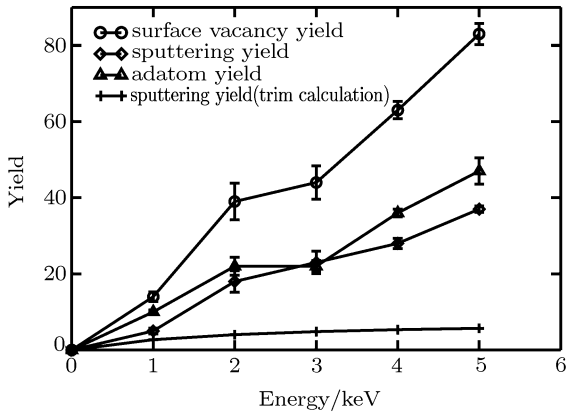


Fig. 4. Yield of sputtered atoms (square), vacancies (circle), interstitials (triangle) and the sputtering yield of trim calculation (cross). The first three yields show linear proportional relationship with incident energy. The trim calculations shows that the sputtering yield of bulk materials is much lower than that of nano-scale materials.

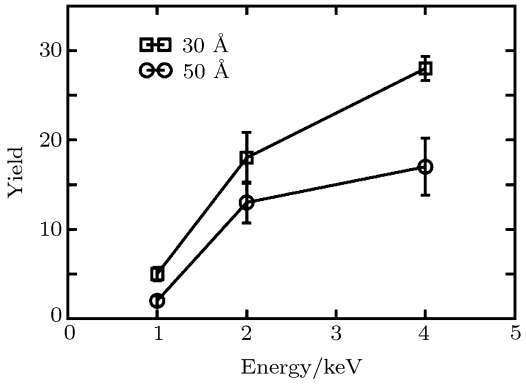


Fig. 5. The sputtering yield of 30 Å diametre (square) nanowire and 50 Å diametre nanowire (circle) under 1 keV, 2 keV and 4 keV ion bombardments. The sputtering yield of 30 nm nanowire is higher than the sputtering yield of 50 nm nanowire.

We used trim program to calculate the sputtering yield of flat copper surface impacted by copper ion with energy from 1 keV to 5 keV. The results are also presented in Fig. 4. The trim calculation shows that the increase of sputtering yield of flat copper surface becomes slow with the increase of incident energy, and is much lower than the sputtering yield of nanowire with the same energy bomdardment. This comparison indicates that the sputtering yield of nano-scale material is higher than that of bulk materials. To verify the impact of nanowire size on sputtering yield, We simulated the sputtering process of 50 Å diametre nanowire under 1 keV, 2 keV, 4 keV ion bombardments. Figure 5 comparing the sputtering yield of 30 Å nanowire and 50 Å nanowire, shows that 30 Å nanowire has higher sputtering yield than 50 Å nanowire.

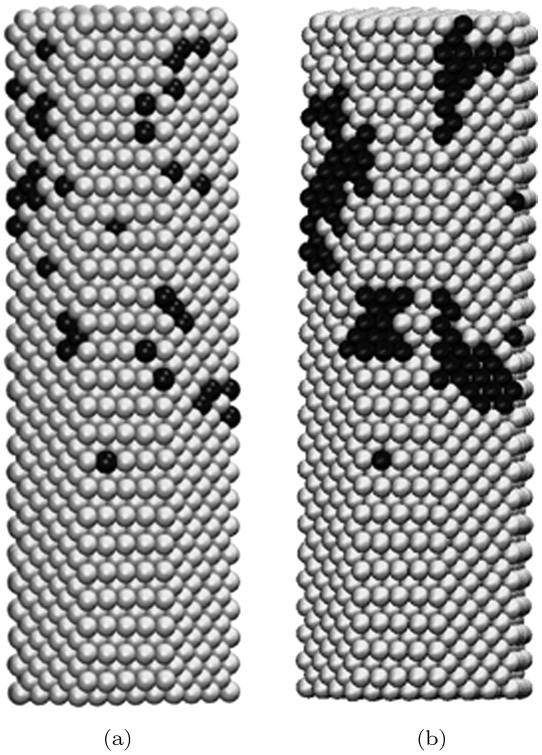


Fig. 6. Comparison of the initial position of sputtered atoms (a) and the final position of surface vacancies (b) under 5 keV-bombardment. 5 keV-bombardment sputtered atoms out of surface all around nanowire, not only on the incident surface. After equilibration, surface vacancies left by sputtered atoms and relocated adatoms accumulated together to form big void cluster on surface of nanowire.

Figure 6(a) shows the initial position of sputtered atoms on nanowire in a 5 keV-bomdardment simulation. We observed three features of the sputtering: (i) sputtered atoms spread around the nanowires. Under 1 keV-bomdardment, the sputtered atoms all came from the side where ion impacted, but under 5 keV-bomdardment, sputtered atoms distributed around the surface of nanowire. Under lower-energetic impact, only atoms on the incident face of ion were sputtered out of the surface, while under higher-energy, the bombardment induced collision cascades can sputter atoms out all around the surface, even the opposite side of incident face. (ii) with the increase of incident

energy, ion can sputter the atoms not only from the first layer, but also the second even the third layer. (iii) with the increase of incident energy, clusters of atoms can be sputtered. We observed that under 1 keV, only single atom was sputtered, while under 3 keV, we observed 2 atoms were sputtered together, and under 5 keV, sputtered cluster composed of 3 atoms were observed. Figure 6(b) presents the distribution of surface vacancy left by sputtered atoms and adatoms. Although the sputtered atoms distribute dispersedly on nanowire, the final surface vacancies were mainly included in four vacancy clusters. The detailed evolution process of vacancy diffusion will be presented later in next part.

3.3. Formation of defects

Energetic ion not only sputteres atoms out of the surface, but also induces displacement cascades, which created plenty of defects including bulk vacancies, interstitials, surface vacancies and adatoms in nanowires. In our simulations, few of 4 keV and 5 keV simulations got bulk defect (vacancy and interstitial), which are less than 2% of all defects. Figure 4 shows the production of defects. Similar to sputtering yield, the adatom and surface vacancy yields are also linear proportional to the incident energies.

Figure 7 demonstrates the evolution of vacancies (bulk vacancies and surface vacancies). Around 0.5 ps, the vacancy yield achieved the maximum value in all simulations. At this moment the lattice of irradiation area is maximumly disordered. Under 1 keV ion bombardment, only a fraction part of area near the incident point was damaged. With the increase of incident energy the depth of lattice damage extended, e.g., under 5 keV ion impact, half part of the nanowire became disordered. 450 vacancies were generated during the process, and most of them are vacancies in bulk. Then the recombination of vacancies and interstitials enhanced by local heat decreased the number of defects. The number of vacanies became constant after 6 ps equilibration. Figure 8 illustrates the recombination processes of vacancies, interstitials and adatoms after 5 keV-bombardment.

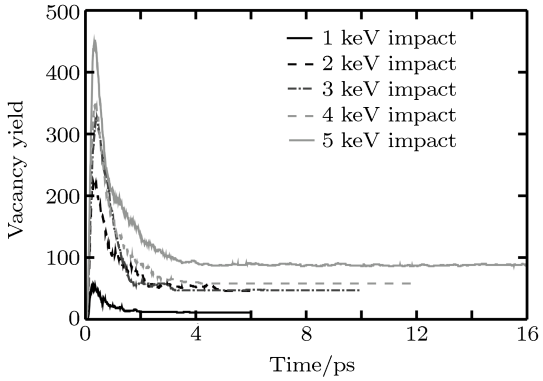


Fig. 7. Evolution of vacancy after ion bombardment. The yield of vacancy achieves the maximum value around 0.5 ps. After 6 ps, the number of vacancies becomes constant. 5 keV ion bombardment caused most vacancies number during irradiation.

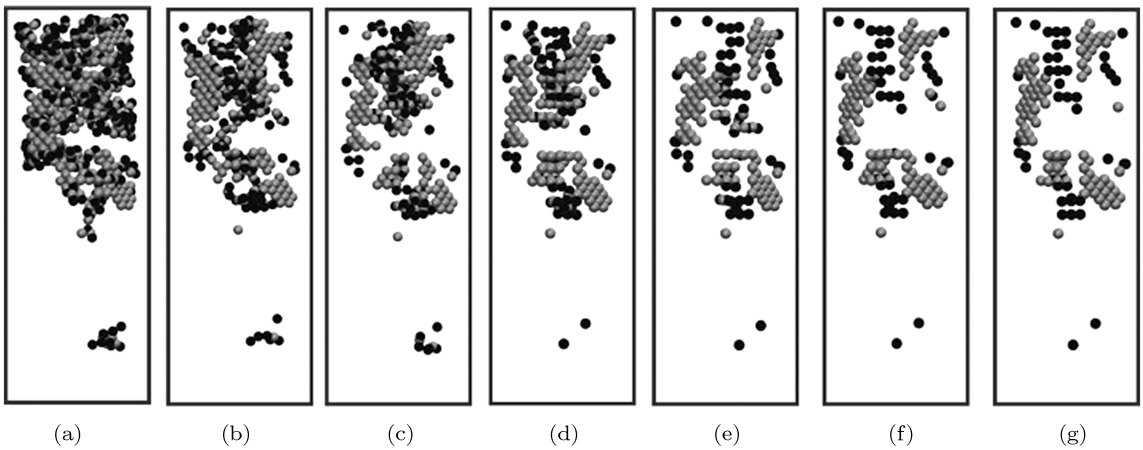


Fig. 8. Recombination process of surface vacancies and adatoms. A large number of surface vacanies and adatoms were created by ion bombardment at the beginning, but most of vacancies and adatoms disapeared due to surface diffusion enhanced by local thermal effect. (a) 0.5 ps, (b) 1 ps, (c) 1.5 ps, (d) 2 ps, (e) 3 ps, (f) 4 ps, (g) 5 ps. The diffusion of defects gradually shows a crystalline surface dependent distribution during recombination process. Vacancies accumulated on ⟨100⟩ plane, while adatoms accumulated on ⟨110⟩ plane.

When number of defects achieved to a constant value at the end of simulation, we found three interesting phenomena of vacancy distribution on nanowire: (i) most of vacancies were observed on the surface of nanowire. With lower-energies impact (1 keV, 2 keV), there were only surface vacancies, and no bulk vacancy was observed. With higher-energy impact, 90% vacancies diffused to the surface. (ii) surface vacancies agglomerated together to form vacancy clusters. Figure 9 shows that higher incident energy not only induced bigger vacancy cluster, but also increased the quantity of vacancy clusters, e.g. a 5 keV-bombardment induced 3 surface vacancy clusters on nanowire. $f_c = N_c/N_F$ presents the fraction of clustered defects, where N_c is the number of defects in clusters of size 2 or more. f_c of vacancy varies from 80% to 95%, while f_c of adatom varies from 60% to 80%. (iii) Most of surface vacancies clusters located on (100) crystal plane, or the cross-section of (100) plane and (110) plane, see Fig. 2. Similar to the distribution of vacancies, most of interstitial defects inside nanowire disappeared after equilibration, and only adatoms on the outermost surface layer were observed in final state of defects. Increase of incident energy induced formation of large adatoms clusters as well as the increase of adatom clusters quantity. Different from surface vacancy, adatom favour the (110) plane more than (100) plane, see Fig. 2.

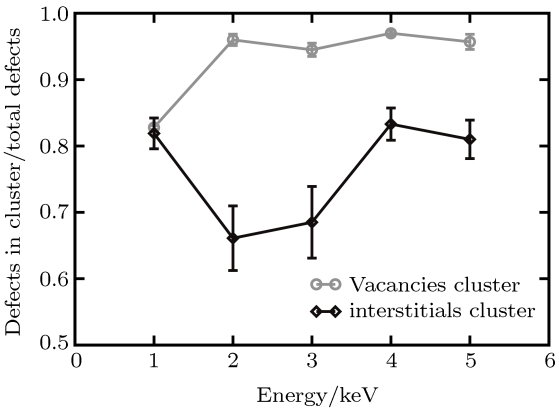


Fig. 9. The fraction of clustered defects. Most vacancies and interstitials caused by irradiation formed defect clusters after equilibration. Fraction of clustered interstitials deviates significantly from the mean.

The clustering of point surface defects on nanowire observed in all simulations shows great dependence on the incident energy and crystal face. As described above, both the size and quantity of surface vacancy clusters and adatom clusters increased with the rise of incident energy. The difference between these two defects clusters is that surface vacancy clusters were observed mostly on (100) plane, while most of adatom clusters were observed on (110) plane. Furthermore, the conformation adopted by adatom cluster is different from the conformation of vacancy cluster, because they formed on difference crystal face. To further understand the mechanism of defects clustering on nanowire caused by irradiation, we look more closely into the details of formation of two defects clusters.

3.3.1. Formation of surface vacancy cluster

Surface vacancies cluster formation involves two steps: (i) single vacancy was created by sputtering atoms out of its lattice or by rolocating atoms onto the outermost surface layer (adatoms). (ii) Vacancy agglomeration. Under 1 keV bombardment, a small 2D surface vacancy cluster including 6 defects was observed on (100) plane. 3D surface vacancy clusters involving 3 atomic layers were induced by high energy bombardment ($\geq$ 2 keV). These surface vacancy clusters always involve both (100) plane and (110) plane, but most part of vacancy clusters are on (100) plane. Figure 10(a) illustrates that vacancy defects formed on (100) plane are always more than those on (110) plane. With the increase of ion energy, the number of surface vacancies on (110) plane decreases, although the total number of surface vacancies increase. High incident energy also induced complicated conformation of clusters, e.g., a stacking fault tetrahedra (SFT) was found under 5 keV bombardment. This SFT involves 15 vacancies and 9 interstitials.

3.3.2. Formation of adatom cluster

Adatom clustering is also determined by two steps: (i) single adatom created by ion impact. (ii) Adatom agglomeration. A large number of adatoms are created on the surface during ion sputtering. After equilibration, these randomly distributed adatoms formed several adatom clusters. Figure 2 demonstrates the conformation of adatom clusters under different energy impacts. Under 1 keV bombardment, clusters including 2 adatoms were observed on (110) plane along $\langle 110 \rangle$ direction. Under 2 keV bombardement, 4 adatoms clustered were observed on (110) plane along $\langle 110 \rangle$ direction. Small clusters of 2 adatoms on (100) plane were also observed. 5 keV bombardment induced 3D stacking adatom cluster

on (110) plane. Figure 10(b) presents that contrary to surface vacancy, adatoms agglomerated on (110) plane more than on (100) plane under energetic impact. With the rise of incident energy, the number of adatoms on the (110) plane slows down, while on (100) plane the number of adatoms grows up rapidly.

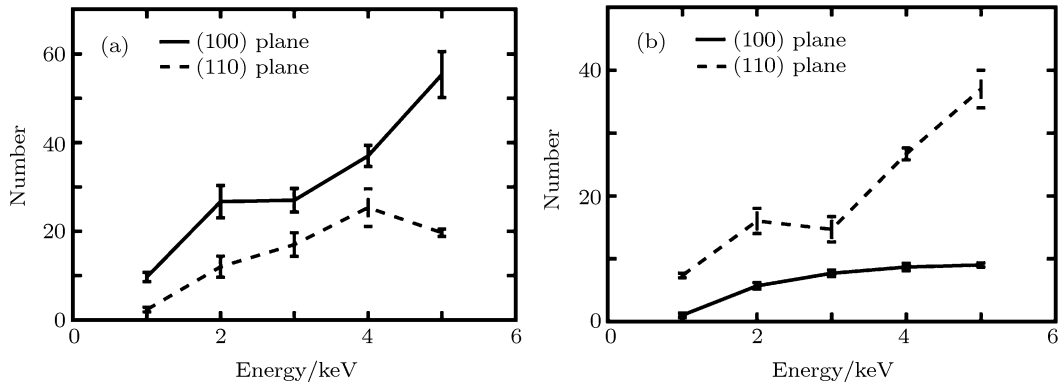


Fig. 10. Distribution of surface vacancies (a) and adatom (b) on two crystalline face. (a) More surface vacances were observed on (100) plane (line) than on (110) plane (dash-line). (b) Contrary to surface vacancies, more adatoms were observed on (110) plane (dash-line) than on (100) plane (line).

4. Discussion

4.1. Big surface-volume ratio of nanowire induces increase of sputtering yield

Our results showed that the sputtering yield of nanowire increases due to its big surface-volume ratio. We found the recoil atoms created in the collision cascade can be sputtered when they move towards the surface with sufficient energy to overcome the surface binding potential barrier. The average value of sputtering yield is dependent on the energy deposition of incident ion and surface curvature. For a flat surface, experiments show that sputtering yield increase slows down with the rise of incident energy.[22] In our simulation, the sputtering yield of ion keeps linearly proportional to the incident energy in range of 1 keV to 5 keV, and its magnitude is much higher than that of bulk materials. The big surface–volume ratio of nanowire results in this increase of sputtering yield efficiency. The influence of increased sputtering yield of nano-scale materials should be taken into concern when we study the irradiation on nano-scale materials.

The physical property change by big surface-volume ratio induced was widely observed in nano-scale materials. For example, with the decrease of nanowire's cross-section, its yield stress is increased.[23] Increase of sputtering yield was also observed in irradiation process of nano-scale materials, but different size and structure result in different sputtering yield.[24] Sputtering modifies the surface morphology by transferring mass out of the target. The irradiation-induced damage of nanomaterials is enhanced by increase of sputtering yield, and differ from one nanostructure to another nanostructure. In other words, the sputtering yield of nanostructure is more sensitive to the specific incident surface and the shape of the target. To determine the ion bombardment effect on specific nanostructure, like nanowire, it is necessary to investigate the size and shape dependent sputtering yield and atomic detailed sputtering process.

4.2. Anisotropic surface diffusion of nanowire

In our simulations, we observed that surface vacancies favour the (100) plane, while adatoms favour the (110) plane. This crystalline surface dependent defects distribution can be understood by the activation energy needed for defects diffusion. The activation

energy for adatom jumping on Cu(100) is 0.425 eV, on Cu(110) and along ⟨110⟩ direction it is 0.292 eV, and on Cu(110) along ⟨001⟩ it is 0.826 eV.[25] The activation energy for the adatom jumping increases through the sequence (110) long bridge, (100), and (110) short bridge. Thus, adatoms have lower energy barrier for jumping on (110) plane along ⟨110⟩ direction than jumping on (100) plane. In that case, more adatoms gather on (110) plane, and recombine with vacancies, or form adatom cluster. Because the energy barrier for adatom jump along ⟨001⟩ direction is very high, we only observed adatom cluster on (100) plane along ⟨110⟩ direction. The activeation energy for vacancy diffusion on Cu(100) is 0.437 eV, on Cu(110) along ⟨110⟩ direction is 0.506 eV, and on Cu(110) along ⟨001⟩ is 0.921 eV respectively.[25] Contrary to adatom, The activation energy for vacancy diffusion on (100) plane is lower than it on (110) plane, so it is easier for vacancies agglomerate on (100) plane than on (110) plane. Also since the activation energy for vacancy diffusion is higher than that for adatom on all crystalline surface, the vacancies are relatively more stable than adatoms so that adatoms diffusion dominates the recombination of defects. The crystalline surface dependent defects distribution results in a crystalline surface dependent surface pattern of nanowire after being irradiated by energetic ion.

5. Conclusions

We preliminarily studied the irradiation damage on copper nanowires by investigating three specific aspects: (i) the relationships between sputtering atoms production and energy of the incident ion , (ii) the atomic details of defect distribution on nanowire, and (iii) the mechanism of defects diffusion on nanowires. Results showed that due to the large surface/volume ratio, the sputtering yield of nanowires is larger than that of bulk materials. The sputtering yield of nanowires is linear proportional to the energy of incident ion in the range of 1 keV to 5 keV. The vacancy defects on the surface gather together to form void cluster mainly on (100) plane, while adatoms mainly aggregate on (110) plane along ⟨110⟩ direction forming adatom clusters. Further researches are needed to study the influence of incident angle and size of nanowire on irradiation damage of nanowire, and the effects of defects on the physical properties of nanowires, like mechanical properties and thermal properties.

Acknowledgement

The authors thank Professor Zhao Zi-Qiang for insightful discussion.

References

[1] Patolsky F, Timko B P, Zheng G and Lieber C M 2007 *MRS-Bulletin* **32** 142
[2] Lu W and Lieber C M 2007 *Nat. Mater.* **6** 841
[3] Kang J W, Seo J J, Byun K R and Hwang H J 2002 *Phys. Rev.* B **66** 125405
[4] Diao J, Gall K and Dunn M L 2004 *J. Mech. Phys. Sol.* **52** 1935
[5] Gu X K and Cao B Y 2007 *Chin. Phys.* **16** 3777
[6] Wen Y, Zhang Y, Zhu Z and Sun S 2009 *Acta Phys. Sin.* **58** 2585 (in Chinese)
[7] Tombrello T A 1987 *Nucl. Instr. Meth. Phys. Res.* B **27** 221
[8] Rusponi S, Boragno C and Valbusa U 1997 *Phys. Rev. Lett.* **78** 2795
[9] Rusponi S, Costantini G, de Mongeot F Buatier, Boragno C and Valbusa U 1999 *Appl. Phys. Lett.* **75** 3318
[10] Ye Z Y and Zhang Q Y 2001 *Chin. Phys.* **10** 329
[11] Ishigami M, Choi H J, Aloni S, Louie S G, Cohen M L and Zettl A 2004 *Phys. Rev. Lett.* **93** 196803
[12] Biersack J P 1987 *Nucl. Instr. Meth. Phys. Res.* B **27** 21
[13] Ritter M, Stindtmann M, Farle M X, Baberschke K 1996 *Surf. Sci.* **348** 243
[14] Xue J M and Imanishi N 2002 *Chin. Phys.* **11** 245
[15] Pan J, Takeda Y, Amekura H, Nakayama Y, Song M and Kishimoto N 2008 *Nanotechnology* **19** 375306
[16] Sun Z H, Wang X X and Wu H A 2008 *J. Appl. Physiol.* **104** 033501
[17] Ziegler J F, Biersack J P and Littmark U 1985 *The Stopping and Range of Ions in Matter* (Oxford: Pergamon Press)
[18] Daw M S and Baskes M I 1984 *Phys. Rev.* B **29** 6443
[19] Mishin Y, Mehl M J, Papaconstantopoulos D A, Voter A F and Kress J D 2001 *Phys. Rev.* B **63** 224106
[20] Osetsky Y N and Bacon D J 2001 *Nucl. Instr. Meth. Phys. Res.* B **180** 85
[21] Eckstein W, Garcia R C, Roth J and Ottenberger W 1996 *Phys. Rev.* B **53** 11376
[22] Eckstein W, Garcia R C, Roth J and Ottenberger W 1993 *Sputtering Data Report IPP* p196
[23] Wu H A, Soh A K, Wang X X and Sun Z H 2004 *Key Eng. Mat.* **261** 33
[24] Jarvi T T, Kuronen A and Nordlund K 2007 *J. Appl. Physiol.* **102** 124304
[25] Stoltze P 1994 *J. Phys.: Condens. Matter* **6** 9495